Research Article

David Jäger*, Christoph Zellmann, Felix Schlatter, and Jean Marc Wunderli

Validation of the sonAIR aircraft noise simulation model

https://doi.org/10.1515/noise-2021-0007
Received Aug 31, 2020; accepted Jan 04, 2021

Abstract: sonAIR is a recently developed aircraft noise simulation model designed for single flight simulation while still being applicable for calculation of entire airport scenarios. This paper presents a rigorous validation exercise, wherein roughly 20'000 single flights were simulated using the 22 currently available sonAIR emission models of turbofan aircraft and compared against noise measurements. The measurements were recorded with the noise monitoring terminals at Zurich and Geneva airport, Switzerland, and with additional microphones installed by the author's institution. Data from 22 measurement positions were analyzed, covering all departure and approach routes at distances from 1.8 to 53 kilometers from the airports. sonAIR was found to be accurate for departures and approaches under different operating conditions and aircraft configuration. The mean overall differences between simulation and measurements were well below ±1 dB in terms of noise event levels, with standard deviations of ±1.7 dB respectively ±2.4 dB, depending on the model type. A few aircraft types that displayed larger deviations are discussed individually. A sensitivity analysis on the input data found the quality and level of detail of the land cover data to be critical for the simulation accuracy. Changes in other input data such as atmospheric profiles and buildings had non-significant impacts.

Keywords: sonAIR, aircraft noise, simulation, validation

***Corresponding Author: David Jäger:** Empa, Laboratory for Acoustics/Noise Control, 8600 Dübendorf, Switzerland;
Email: david.jaeger@empa.ch
Christoph Zellmann: Empa, Laboratory for Acoustics/Noise Control, 8600 Dübendorf, Switzerland;
Email: christoph.zellmann@empa.ch
Felix Schlatter: Grolimund + Partner AG, 3006 Bern, Switzerland;
Email: felix.schlatter@grolimund-partner.ch
Jean Marc Wunderli: Empa, Laboratory for Acoustics/Noise Control, 8600 Dübendorf, Switzerland;
Email: jean-marc.wunderli@empa.ch

Abbreviations

FDR	flight data recording
GVA	Geneva airport
$L_{AE,tg}$	A-weighted sound exposure level over tg
$L_{AS,max}$	A-weighted maximum sound level
NMT	noise monitoring terminal
$N1$	rotational speed of low pressure fan
tg	time with sound level above threshold
ZRH	Zurich airport

1 Introduction

Aircraft noise calculations are well-established for land-use planning and management worldwide. Harmonized best practice approaches such as ICAO Doc. 9911 [1] and ECAC Doc. 29 [2] are designed to reproduce long-term averages. However, to calculate single flights or new flight procedures, the demands on the model accuracy are higher. There are scientific semi-empirical models such as ANOPP [3], CARMEN [4], SOPRANO [5] and PANAM [6] for this application, but their drawbacks are the demand for very detailed input data (*e.g.* primary jet speed or airflow mass) and their limited accessibility to a wide user base. Yet, these scientific models are the only choice to assess novel aircraft designs and technology.

The sonAIR aircraft noise simulation tool was developed at the author's institution to bridge the gap between these two approaches [7–9]. It was designed to accurately simulate noise emission and propagation of single flights with a high level of detail, while still being applicable for noise mapping of entire airport scenarios. The model design was held flexible in order to allow for different levels of detail of the input parameters. The sonAIR model design allows the extension of the current emission lookup tables by incorporating existing noise databases from external sources or simulations done with one of the scientific tools described above. This allows the noise assessment of novel aircraft designs and technology, as demonstrated in [10].

To ensure that aircraft noise models produce realistic noise contours, a systematic comparison of simulations and independent measurements is necessary. Such validation efforts were conducted in the past for certain noise models such as ANCON in the United Kingdom [11–13] and FLULA2 in Switzerland [14, 15]. However, not all of those publications show complete results for all available aircraft types. Some effort was also taken to test scientific aircraft noise models, but these are limited to a few exemplary aircraft types and to comparisons between different tools without validation against measurements [16, 17]. Other widely used aircraft noise models offer no readily available validation data at all.

The publication of complete and detailed validation results is essential for the transparency and credibility of any aircraft noise model. We already presented a first sonAIR validation case study, where simulations were compared to independent measurements of approaches to Schiphol airport in the Netherlands. This small-scale validation revealed good agreement between simulation and measurements, with mean deviations of -0.2 ± 1.1 dB in terms of the sound event level [18]. However, a full validation requires a much larger set of independent measurement data, covering departures and approaches under different operating conditions, aircraft configuration and in different distances to the airport.

This article presents the results of a validation exercise of the sonAIR aricraft noise model, based on a large number of operational noise measurements at the airports of Zurich and Geneva, Switzerland, over an entire year. It quantifies the accuracy of the 22 currently available sonAIR emission models of turbofan aircraft. Section 2 gives an overview of sonAIR and the applied validation method, including a detailed description of the measurements, input data and simulation. Section 3 shows the validation results, which are then discussed in-depth in section 4. Finally, a short conclusion and outlook is given in section 5.

2 Data and methods

2.1 sonAIR aircraft noise model

The sonAIR aircraft noise model consists of two separate modules: the sound emission is calculated based on a set of linear regression equations derived from an extensive measurement campaign of real-world air traffic. The propagation calculation is based on physical definitions of sound propagation through the air. Both models are defined for one-third octave bands.

The emission model is further subdivided into engine and airframe noise. The engine noise levels are modeled as the sum of a source term and radiation angle terms (Equation 1).

$$\widehat{L}_{em,eng}(f) = \underbrace{\widehat{L}_{0,eng}}_{\text{source term}} + \underbrace{\Delta\widehat{L}_{\theta,eng} + \Delta\widehat{L}_{\varphi,eng}}_{\text{radiation angle terms}} \tag{1}$$

The source term for engine noise includes the intercept L_{e0} along with the Mach number Ma and the rotational speed of the low pressure compressor ($N1$) multiplied with their coefficients a_{e1}, b_{e1} and b_{e2} (Equation 2).

$$\widehat{L}_{0,eng} = L_{e0} + a_{e1} \cdot Ma + b_{e1} \cdot N_1 + b_{e2} \cdot N_1^2 \tag{2}$$

The radiation angle terms for engine noise consist of two summands: the first describes the interaction of $N1$ with the polar angle θ (Equation 3). The second defines the interaction of $N1$ with the azimuth angle φ, whereby symmetry of φ in the vertical plane is assumed (Equation 4). The engine noise therefore features a three dimensional directivity pattern, changing its shape with $N1$. The corresponding model coefficients are $k_{e,j}$ to $p_{e,j}$ with index j for each interaction.

$$\begin{aligned}\Delta\widehat{L}_{\theta,eng} = (&k_{e,j} \cdot \cos\theta + l_{e,j} \cdot \cos 2\theta \\ &+ m_{e,j} \cdot \sin\theta + n_{e,j} \cdot \sin 2\theta) \\ &\cdot (1 + N1 + N1^2)\end{aligned} \tag{3}$$

$$\Delta\widehat{L}_{\varphi,eng} = (o_{e,j} \cdot \sin\varphi + p_{e,j} \cdot \sin 2\varphi) \cdot (1 + N1) \tag{4}$$

Like the engine model, the airframe noise is modeled as the sum of a source term and a radiation angle term (Equation 5).

$$\widehat{L}_{em,afm}(f) = \underbrace{\widehat{L}_{0,afm}}_{\text{source term}} + \underbrace{\Delta\widehat{L}_{\theta,afm}}_{\text{radiation angle term}} \tag{5}$$

The source term for the airframe model is formulated in two versions, depending on the level of detail of the available input data. Advanced airframe noise models (hereinafter referred to as *full models*) account for the aircraft configuration, *i.e.* the position of the flaps (FH), speedbrakes (SB) and the landing gear (LG), as well as the aircraft Mach number Ma and the air density ρ. These variables are included in the airframe noise source term along with their frequency-dependent coefficients a_{a1} to e_{a3}, the procedure ($Proc$) and the intercept L_{a0} as described in Equation 6. To generate these models, full flight data recordings (FDR) containing information on the aircraft configuration at every point of the trajectory are required, in order to determine

the effects of each variable by time-wise correlation of the FDR data with noise measurements on the ground.

$$\begin{aligned}\widehat{L}_{0,afm} = {} & L_{a0} + a_{a1} \cdot lMa + Proc \cdot (a_{a2} + a_{a3} \cdot lMa) \\ & + b_{a1} \cdot l\rho + LG \cdot (c_{a1} + c_{a2} \cdot Proc + c_{a3} \cdot lMa) \\ & + \sum_{j=1}^{4} FH_j \cdot (d_{a1j} + d_{a2j} \cdot LG + d_{a3j} \cdot Proc) \\ & + SB \cdot (e_{a1} + e_{a2} \cdot LG + e_{a3} \cdot lMa)\end{aligned} \quad (6)$$

Reduced airframe noise models (hereinafter referred to as *reduced models*) do not explicitly account for the aircraft configuration. They can be generated without access to FDR data. The corresponding airframe source term is therefore shortened to Equation 7.

$$\widehat{L}_{0,afm} = L_{a0} + a_{a1} \cdot lMa + Proc \cdot (a_{a2} + a_{a3} \cdot lMa) + b_{a1} \cdot l\rho \quad (7)$$

The radiation angle term for the airframe model only depends on the polar angle θ without any interactions (Equation 8). The coefficients for the airframe directivity are k_a to n_a. The airframe model therefore features a two dimensional directivity pattern, assuming axially symmetric radiation along the longitudinal axis.

$$\Delta\widehat{L}_{\theta,afm} = k_a \cdot \cos\theta + l_a \cdot \cos 2\theta + m_a \cdot \sin\theta + n_a \cdot \sin 2\theta \quad (8)$$

For further detail on the emission model, see [7–9].

The sound propagation calculation is accounting for geometrical spreading, air absorption according to ISO 9613-1 [19] with an extension for broadband tones according to [20], shielding effects as given in ISO 9613-2 [21] or proposed by Pierce [22], foliage attenuation according to the annex of ISO 9613-2 [21], ground reflections and meteorological effects. Air absorption is calculated using average values of temperature, humidity and pressure for sections of 100 m height of a stratified atmosphere up to 10 km. Representative air absorption coefficients per one-third octave band are calculated for each section and summed up. Ground reflections are calculated for spherical waves over flat and homogeneous ground according to [23], with an extension for uneven terrain and varying ground properties. Thereby, the frequency dependent ground impedance model by Delany and Bazley [24] is used with the flow resistance of the ground as single free parameter. Meteorological effects are calculated based on arbitrary vertical sound speed profiles as input, using a ray tracing algorithm that yields variations of barrier effects as well as level decreases in acoustical shadow zones as results [25]. For further details on the sound propagation calculation, see [9].

During the initial development phase of sonAIR, a set of 19 emission models was generated based on an extensive measurement campaign of air traffic at Zurich airport in 2013 and 2014 [7, 8]. These models are hereinafter referred to as *published models*. For flights operated by Swiss Airlines, FDR data was available. The corresponding six Swiss aircraft types are therefore available as full models: Airbus A319, A320 and A321 with engine type CFM56-5B; Airbus A333 with engine type TRENT7; Airbus A343 with engine type CFM56-5C; and BAE Systems Avro RJ100 with engine type LF507 (since Swiss Airlines were phasing out their RJ100 fleet during the validation measurements in 2016 and 2017, the corresponding model was not validated). The remaining 13 models are available as reduced models. As some reduced models can be applied to an entire family of aircraft (*e.g.* the emission model A32X_CFM56-5A which is applicable for the A319, A320 and A321), this set of models covers 31 individual aircraft-engine-combinations.

Since the initial sonAIR project, some updates and extensions were implemented. The airframe noise models of the Airbus A320 family were updated to account for the airflow deflectors that were retrofitted onto the A320 fleets of most large airlines [26]. These deflectors suppress two dominant cavity tones that were still present in the initial sonAIR source measurements, necessitating a model update. Furthermore, the change of the aircraft fleet operating at large airports requires the ability to efficiently and timely update the sonAIR aircraft database. To this end, a setup of mobile, energy self-sufficient, remote-controlled noise monitoring terminals was developed in close collaboration with NTi Audio [27]. This setup was used to update the model database with the three newly acquired aircraft types of Swiss Airlines (Bombardier CS100 and CS300, rebranded as Airbus A220-100 and A220-300, and Boeing B777-300ER). These additional emission models are hereinafter referred to as *new models*.

2.2 Parameter estimation

sonAIR requires information on the engine rotational speed $N1$ as input data. Yearly noise calculations are based on radar data, which does not provide any information on engine settings. Therefore, a new approach to estimate $N1$ from radar data was developed at the author's institution [28]. It treats departures and approaches separately.

The departure is split into the two phases *take-off thrust* and *climb thrust*. Take-off thrust is usually a continuously reduced thrust setting that is held constant until reaching the cutback altitude. The cutback altitude depends on airport or airline procedures, in Switzerland it is prescribed at 1500 ft above airport elevation.

Based on either FDR data or acoustically derived $N1$-data [29], a regression model was established at different

altitude levels. For reduced take-off thrust, the altitude dependent estimation of $N1$ accounts for the constant aircraft mass m, the mean angle of climb $\overline{\gamma}$ of the initial climb phase before cutback, and T_h as the outside temperature at the actual altitude h (Equation 9).

$$N1_h^2 = f(m, \overline{\gamma}, T_h) \tag{9}$$

In case that no aircraft mass is available, the lift-off velocity v_{LO} is applied as a proxy [2] (Equation 10).

$$N1_h^2 = f(v_{LO}, \overline{\gamma}, T_h) \tag{10}$$

After cutback, the engine usually operates at a constant thrust level. As the density and temperature decrease with altitude, $N1$ slightly increases with altitude. For continuous climb, a different regression model is applied to estimation $N1$, which is again established for different altitude levels (Equation 11).

$$N1_h = f(|T_h|) \tag{11}$$

Thereby, $f(|T_h|)$ describes the dependency of the needed $N1$ for the constant thrust rating and considers the limitation of overheating of the turbine as a function of the outside air temperature and altitude.

Some wide-body aircraft such as the A333 with TRENT772 engines provide two de-rated climb ratings for standard flight procedures. The de-rated climb rating is detected via a balance of the total energy during continuous climb. In the case of two or more ratings, the regression model is established individually for each de-rated climb rating.

This methodology is built on FDR data from Swiss Airlines or $N1$-data from the sonAIR measurements [8]. If the database was not sufficient, only a median $N1$-profile was generated. This way, the parameter estimation can be performed for each available aircraft noise emission model, but at different levels of accuracy.

For approaches, no such methodology could be developed to reliably estimate $N1$. Therefore, approaches are modelled via median $N1$-profiles, which are based on the air traffic at Zurich airport from 2013 and 2014. For more detail on the $N1$ estimation methodology, see [28].

2.3 sonAIR validation

The validation process consists of a comparison of sonAIR single flight simulations with independent measurements. Full models and reduced models were validated separately, since they require different levels of detail in terms of input data. A large set of measurement data was available from the airports of Zurich and Geneva in Switzerland, recorded by the airport-operated noise monitoring terminals (NMT). The main datasets used for the validation covered all regular flights during the year 2016. Since the Bombardier CS100 and CS300 were introduced in the second half of 2016, NMT data from 2017 was used for their validation.

In addition, data recorded during a measurement campaign carried out in autumn of 2017 by the author's institution in larger distances to Zurich airport was used, containing measurements of approaches in clean and partial configuration.

2.3.1 Measurement layout

The NMT network of Zurich airport consists of 14 fixed terminals which are located at distances of one to eight kilometers from the airport (NMTs 1 to 14; see Figure 1). The NMTs are distributed below all departure and approach routes. The omnidirectional microphones are installed on pylons of 3.5 to 9 meters height on top of rooftops located in inhabited areas.

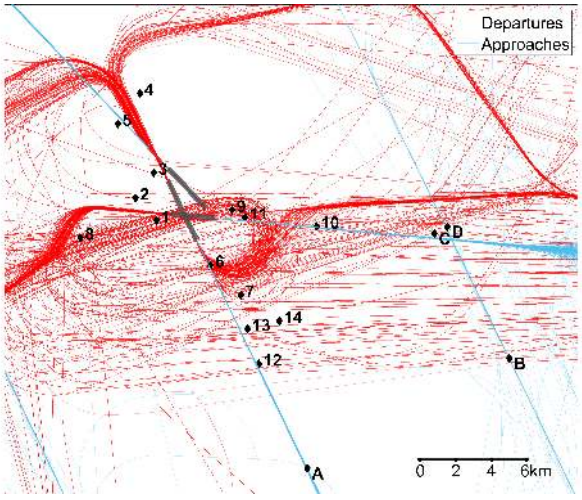

Figure 1: Measurement positions at Zurich airport (NMTs 1-14 and additional measurement points A-D) with flight tracks.

The NMT network in Zurich covers all important flight phases during departure. However, approaches are only recorded within the last few kilometers before touchdown, where the airplanes are typically fully configured for landing. To validate the sonAIR full models in earlier approach phases with clean or partial configuration, we carried out an additional measurement campaign at Zurich airport in autumn of 2017. Four measurement stations were installed at distances between 13 and 53 kilometers from touchdown (measurement stations A to D; see Figure 1). The omnidi-

rectional microphones were mounted on pylons of six to ten meters height in places with minimal obstruction and background noise contamination.

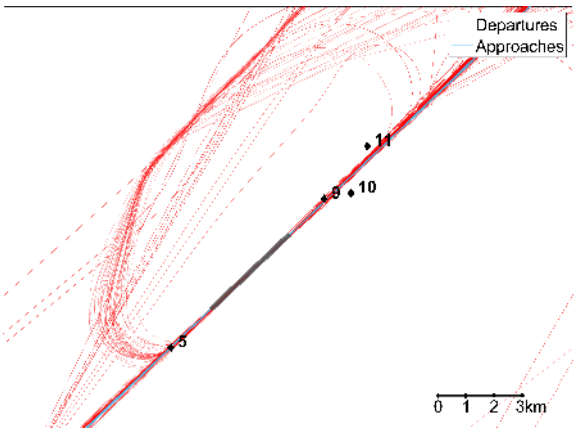

Figure 2: NMT positions at Geneva airport with flight tracks.

Geneva airport has only one runway. Consequently, the NMT network consists of only four terminals underneath the two main directions for departure and approach (Figure 2). As in Zurich, the microphones are installed on pylons on top of rooftops, at distances between 1.8 and 4.2 kilometers from the airport.

During the result analysis, we noticed a systematic overestimation of the measurements at NMT5 in Geneva by roughly 2 dB with both full and reduced models. This is by far the largest deviation observed at any single measurement position in Geneva or in Zurich, despite the fact that NMT5 is located directly underneath the flight paths without any particularly challenging propagation geometries. Since [14] describes similar problems with this particular measurement position, we assume a general problem with Geneva NMT5. Either the measurement equipment was faulty or it was inadequately calibrated. We therefore argue that NMT 5 cannot adequately represent the validation test case and excluded it from the analysis presented in section 3.

2.3.2 Measurement data processing

Both NMT systems automatically detect the aircraft noise events by using individual and time-dependent noise thresholds or dynamic background noise determination. In addition, the measurements are correlated with radar data and flight plan data to filter out non-aircraft noise events. During post processing, the airports further verify the resulting noise events and manually correct for events which contain unwanted noise (road noise, strong winds etc.).

The final dataset consists of a list of noise events, each assigned to a flight number, a noise terminal and the time of flyover. Each event includes information about the maximum A-weighted sound pressure level $L_{AS,max}$, the A-weighted sound exposure level $L_{AE,tg}$ integrated over the time interval tg during which the level was above a set threshold, and the corresponding threshold. Full audio recordings were not available, therefore we could not implement additional quality control measures.

The additional measurement stations A to D in Zurich recorded a continuous audio signal daily between 6 AM and 11 PM. This signal was cut into noise events based on temporal matching with flight plan data. All events were checked for validity; events with severe background noise contamination were excluded from further analysis.

2.3.3 Position data

Depending on the model, one of two sources for position data was used. The full models, which encompass the current fleet of Swiss Airlines, were validated using flight data recordings (FDR) acquired from Swiss Airlines. Aside from the position information, these datasets include all necessary inputs such as flaps and gear position, $N1$, Mach number and air density. The reduced models were validated using radar data for position information and as the basis to estimate $N1$ employing the methodology described in section 2.2.

2.3.4 Selection of noise events

Acquiring the FDR data to simulate all measured flights would have been too expensive. Therefore a subset of the available noise measurements was generated. In a first step, the noise event lists were extended with weather data in order to exclude events recorded during precipitation or strong wind conditions (wind speed above 5 m/s). About one fifth of the total number of noise events were hereby excluded, 14% due to precipitation and 8% due to strong wind conditions (2% intersecting). Thus, the models were explicitly not validated for those weather situations.

Next, a subset of the remaining noise events was selected for simulation. Since a random choice would only represent the most frequent take-off masses and atmospheric conditions, we applied a stratified selection process. The available range of take-off masses of a specific aircraft type was split into 20 equal bins. From each bin, a fixed

number of flights was randomly chosen for every route. The same approach was then used for the available ranges in air temperature and air humidity. This method increases the influence of statistical fringe cases and ensures that the entire range of take-off masses, air temperature and humidity was validated, making it the toughest possible test case. Up to 210 noise events were selected per aircraft-engine-combination.

Finally, the noise events were grouped into flights carried out by Swiss Airlines and into all other airlines. The first group is available in sonAIR as full models. The flights operated by other airlines were mostly available as reduced models and were therefore validated separately from the Swiss types. In total, 4'892 noise events from 2'135 flights carried out by eight different aircraft types were used to validate the full models. For the reduced models, 15'434 noise events from 6'653 flights carried out by 31 different aircraft-engine combinations were used.

2.3.5 Simulation

Each selected noise event was simulated as a single flight and evaluated at the corresponding measurement position. sonAIR calculates full level-time histories for each noise event. From these, the maximum A-weighted sound pressure level $L_{AS,max}$ and the A-weighted sound exposure level $L_{AE,tg}$ were calculated using the event-specific noise thresholds provided in the NMT noise event list.

To characterize the sound reflection on the ground, a digital terrain model and surface properties based on the official surveying of the cantons Zurich and Geneva were used as input. Meteorological influences were accounted for by using COSMO1 profiles of the atmosphere (https://www.meteoswiss.admin.ch/home/measurement-and-forecasting-systems/warning-and-forecasting-systems/cosmo-forecasting-system.html).

Large-scale aircraft noise simulation typically ignores buildings. In this specific validation case, however, the focus lies on the specific levels at the exact positions of the measurement stations, which were located on rooftops in densely built-up areas. Therefore, a vectorized building dataset based on swissBUILDINGS3D (https://shop.swisstopo.admin.ch/en/products/landscape/build3D2) was used as additional input to account for shielding effects of large nearby buildings. However, sonAIR is currently not able to account for reflections on the building facades and rooftops. The facade reflections could be neglected in this case, but as the NMT stations were mostly installed on buildings, rooftop reflection needed to be considered. To that end, the buildings which have NMTs installed on their roofs were extracted from a digital surface model and manually pasted into the digital terrain model, effectively making them a terrain feature. This allowed the substitution of rooftop reflections by calculating ground reflection at the rooftop level.

2.3.6 Sensitivity analysis on input data

The main simulations presented in this study used the best available input datasets. This level of detail might be unavailable or too costly in terms of calculation time for operational noise mapping. A sensitivity analysis was performed to quantify the influence of each input dataset on the overall simulation performance. The simulation was therefore re-calculated three times, each time implementing one of the following changes in input data:

1. Replacing the high detail cantonal surveying land cover data with widely available, coarser data based on 1:25'000 scale national maps (Vector25; https://shop.swisstopo.admin.ch/en/products/maps/national/vector/smv25).
2. Omitting the vectorized building dataset.
3. Replacing the COSMO1 atmospheric profiles (sonAIR METEO mode) with a uniform mean atmosphere with $T = 14^{\circ}C$, $p = 1000\,mbar$ and relative humidity of 60% (sonAIR BASIC mode).

3 Results

The simulated event levels $L_{AE,tg}$ and maximum levels $L_{AS,max}$ were compared individually with the corresponding measurements. The results were then grouped by emission model and procedure (departure or approach). This analysis was done separately for the full models and the reduced models. The numeric results are shown in terms of mean differences (simulation minus measurement) and corresponding standard deviation.

3.1 Full models

4'892 noise events from 2'135 individual flights were evaluated for the validation of the full models. The scatterplot in Figure 3 displays the direct comparison of measured and calculated event levels from all noise events. The numeric results, evaluated over all available measurement points in Zurich and Geneva except GVA NMT5 (as discussed above), are listed in Table 1. Averaged over all available measure-

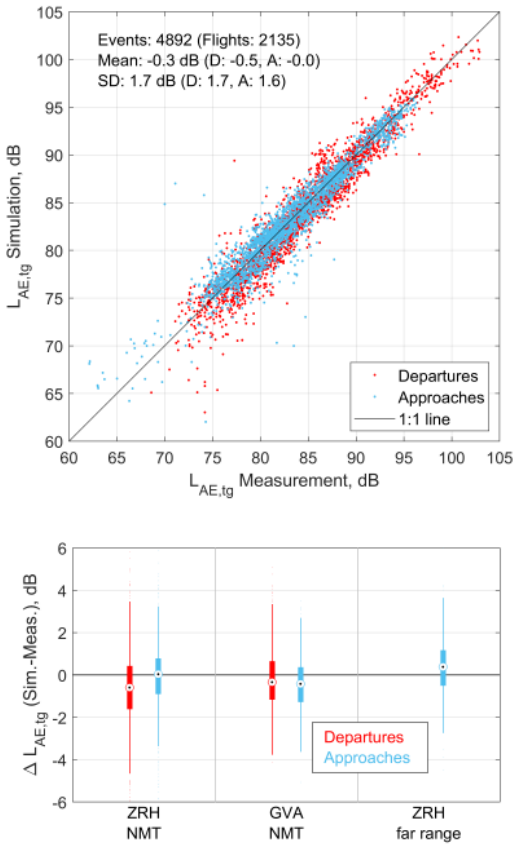

Figure 3: Comparison simulation vs. measurements for full models. Top: Scatterplot with all measurements (ZRH and GVA combined), grouped by procedure (D: Departure; A: Approach; SD: Standard deviation). Bottom: Box-whisker-plots of the measurements, grouped by measurement origin and procedure.

ments, types and procedures, the full models could reproduce the measurements with a $\Delta L_{AE,tg}$ of −0.3 ± 1.7 dB.

At Zurich airport, 3'911 noise events from 1'758 individual flights were evaluated. The results show good agreement between simulation and measurement, with $\Delta L_{AE,tg}$ = −0.4 ± 1.8 dB. A subdivision by procedure demonstrated very close agreement during approach with $\Delta L_{AE,tg}$ = −0.1 ± 1.8 dB. The departures showed a slight underestimation of −0.6 ± 1.8 dB (see box-whisker-plots in Figure 3). A further subdivision of the results by aircraft type showed comparable performances for all validated full models.

The evaluation of the $L_{AS,max}$ (not shown) displayed similar trends, but with larger underestimation of the measurements. The difference in $L_{AS,max}$ is −1.0 ± 2.0 dB, with departures again showing stronger underestimation than the approaches.

At Geneva airport, 981 noise events from 377 flights were evaluated. The simulation matched the Geneva measurements well, with $\Delta L_{AE,tg}$ = −0.3 ± 1.4 dB. Departures

Table 1: Differences between simulation and measurements (ZRH and GVA combined) for all full models, separated into departures (D) and approaches (A). N: number of noise events; SD: standard deviation.

Aircraft	Engine	Emission model	Proc	N	Mean	SD
A319	CFM56-5B	A319_CFM56-5B	D	269	−1.0	1.5
			A	333	−0.2	1.6
A320	CFM56-5B	A320_CFM56-5B	D	315	−0.7	1.7
			A	431	0.1	1.6
A321	CFM56-5B	A321_CFM56-5B	D	327	−0.5	1.6
			A	444	0.6	1.2
A333	TRENT7	A333_TRENT7	D	238	−0.9	1.4
			A	293	−0.3	1.6
A343	CFM56-5C	A343_CFM56-5C	D	300	−0.3	1.9
			A	222	0.2	1.2
B77W	GE90-115B	B77W_GE90-115B	D	382	0.4	1.5
			A	283	−0.7	1.4
BCS1	PW1500G	BCS1_PW1500G	D	303	−0.5	1.8
			A	234	−0.2	1.9
BCS3	PW1500G	BCS3_PW1500G	D	292	−1.2	1.6
			A	226	−0.1	2.1
Total			**D**	**2426**	**−0.5**	**1.7**
			A	**2466**	**0.0**	**1.6**
			all	**4892**	**−0.3**	**1.7**

matched very well (−0.1 ± 1.5 dB), while the approaches showed a slight underestimation (−0.4 ± 1.2 dB; see box-whisker-plots in Figure 3). All eight aircraft types achieved comparable results.

The evaluation of the $L_{AS,max}$ (not shown) displayed slightly larger underestimation of the measurements, with $\Delta L_{AS,max}$ = −0.5 ± 1.5 dB.

3.2 Reduced models

The validation dataset for the reduced models consisted of 15'434 noise events from 6'654 flights. The selection of flights explicitly excluded flights from Swiss Airlines. The validation of the reduced models used NMT measurements only; no measurements from the additional measurement points A to D were available for these types.

The scatterplot in Figure 4 displays the direct comparison of measured and calculated event levels from all noise events from Zurich and Geneva combined. The numeric results, evaluated over all available measurement points in Zurich and Geneva except GVA NMT5 (as discussed above), are listed in Table 2. Averaged over all available measurements, types and procedures, the reduced models reproduced the measurements with $\Delta L_{AE,tg}$ = −0.2 ± 2.4 dB.

At Zurich Airport, 10'307 noise events from 4'630 flights were evaluated. The average over all reduced models at Zurich airport shows good agreement between simulation and measurements, with $\Delta L_{AE,tg}$ = −0.4 ± 2.6 dB. The

Table 2: Differences between simulation and measurements (ZRH and GVA combined) for all reduced models, separated into departures (D) and approaches (A). N: number of noise events; SD: standard deviation.

Aircraft	Engine	Emission model	Proc	N	Mean	SD
A319	CFM56-5B	A319_CFM56-5B	D	536	0.4	2.2
			A	362	1.9	1.6
A320	CFM56-5B	A320_CFM56-5B	D	226	0.0	2.0
			A	141	0.7	1.6
A321	CFM56-5B	A321_CFM56-5B	D	326	−0.6	2.3
			A	344	0.5	1.6
A333	TRENT7	A333_TRENT7	D	581	−1.0	3.3
			A	367	−0.3	1.8
A343	CFM56-5C	A343_CFM56-5C	D	304	0.5	2.5
			A	242	0.6	1.9
A319	CFM56-5A	A32X_CFM56-5A	D	321	0.0	1.6
			A	353	−0.3	1.7
A319	V2500	A32X_V2500	D	444	0.1	1.7
			A	310	1.4	1.9
A320	CFM56-5A	A32X_CFM56-5A	D	344	−0.7	1.3
			A	301	−0.6	1.4
A320	V2500	A32X_V2500	D	315	−0.7	1.8
			A	186	0.8	1.9
A321	V2500	A32X_V2500	D	214	−3.2	1.9
			A	119	0.9	2.2
A388	GP7270	A388_GP7270	D	165	−1.0	2.0
			A	193	4.2	3.2
A388	TRENT9	A388_TRENT9	D	60	0.2	2.6
			A	123	−0.7	1.9
B733	CFM56-3	B737_CFM56-3	D	272	−0.1	2.0
			A	131	−1.0	1.2
B734	CFM56-3	B737_CFM56-3	D	195	−0.4	2.1
			A	257	−1.1	1.3
B735	CFM56-3	B737_CFM56-3	D	338	−0.7	1.6
			A	206	−1.1	1.2
B736	CFM56-7B	B737_CFM56-7B	D	246	1.4	2.0
			A	224	−0.8	2.2
B737	CFM56-7B	B737_CFM56-7B	D	267	−0.4	2.2
			A	255	−0.8	1.8
B738	CFM56-7B	B737_CFM56-7B	D	323	−1.2	2.3
			A	243	−1.3	2.0
B739	CFM56-7B	B737_CFM56-7B	D	214	−2.4	2.0
			A	208	−1.9	2.2
B762	CF6-80C2	B76X_CF6-80C2	D	11	2.1	2.7
			A	18	4.8	1.7
B763	PW4060	B763_PW4060	D	261	−0.7	2.4
			A	143	−0.5	1.6
B763	CF6-80C2	B76X_CF6-80C2	D	249	−0.7	2.6
			A	265	2.2	2.2
B764	CF6-80C2	B76X_CF6-80C2	D	242	−1.0	2.2
			A	239	2.2	2.4
CRJ7	CF34-8C5	CRJ9_CF34-8C5	D	343	−0.3	1.9
			A	187	−0.4	1.4
CRJ9	CF34-8C5	CRJ9_CF34-8C5	D	230	−0.3	1.5
			A	297	−0.9	1.6
CRJX	CF34-8C5	CRJ9_CF34-8C5	D	68	−1.1	1.4
			A	41	−1.9	1.3
E170	CF34-8E	E170_CF34-8E	D	187	−0.1	2.2
			A	178	−0.1	2.2
E190	CF34-10E	E190_CF34-10E	D	477	−1.2	1.9
			A	359	−0.5	1.6
E195	CF34-10E	E190_CF34-10E	D	102	−0.5	1.4
			A	102	−0.7	1.1
F100	TAY650-15	F100_TAY650-15	D	472	−2.0	2.2
			A	312	0.2	3.1
FA7X	PW307	FA7X_PW307	D	215	−0.3	3.2
			A	180	0.5	2.6
Total			**D**	**8548**	**−0.6**	**2.3**
			A	**6886**	**0.2**	**2.3**
			all	**15434**	**−0.2**	**2.4**

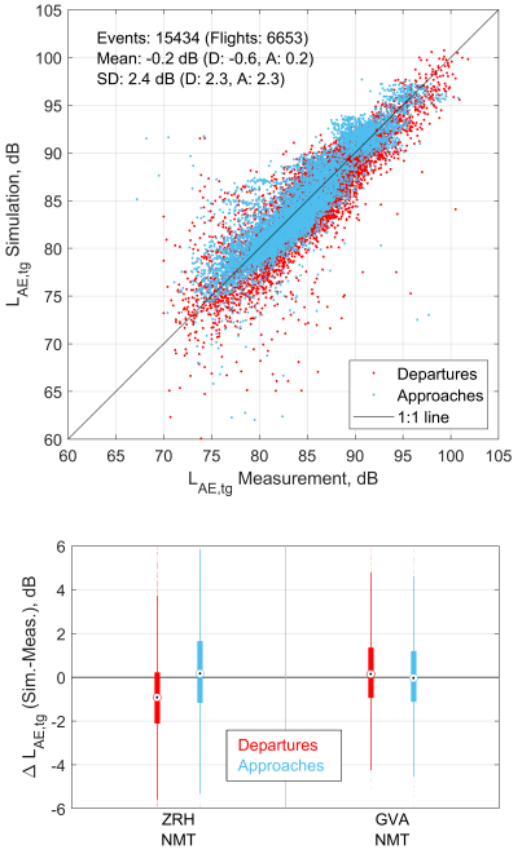

Figure 4: Comparison simulation vs. measurements for reduced models. Top: Scatterplot with all measurements, grouped by procedure (D: Departure; A: Approach; SD: Standard deviation). Bottom: Box-whisker-plots of the measurements, grouped by measurement origin and procedure.

slight underestimation is again mainly caused by the departures ($\Delta L_{AE,tg} = -0.9 \pm 2.4$ dB), whereas the approaches match well ($\Delta L_{AE,tg} = +0.3 \pm 2.6$ dB; see box-whisker-plots in Figure 4). The standard deviation is 0.7 dB larger than that observed with the full models.

As with the full model validation, the $L_{AS,max}$ (not shown) displayed larger underestimation of the measurements in Zurich. The difference in $L_{AS,max}$ is -1.1 ± 2.6 dB, with departures again showing larger underestimation than approaches.

At Geneva airport, 5'127 noise events from 2'024 flights were evaluated. The reduced models achieved slightly better results than in Zurich, with a $\Delta L_{AE,tg}$ of $+0.2 \pm 1.8$ dB (see box-whisker-plots in Figure 4). The maximum level (not shown) was reproduced well, with a $\Delta L_{AS,max}$ of 0.0 ± 2.2 dB.

3.3 Sensitivity analysis on input data

Using the coarser Vector25 dataset as land cover input led to an overestimation of the simulated sound exposure levels by roughly 0.7 dB. The cumulative effect of omitting the 3D building dataset on the entire validation was less than 0.1 dB. The mean differences between the simulations in METEO and BASIC mode with less than 0.1 dB were equally insignificant.

4 Discussion

4.1 Measurement uncertainties

The differences between simulation and measurements given in section 3 on their own already confirm the good model performance of sonAIR, especially considering that the validation is done on the basis of single events, which scatter more pronounced than yearly averaged equivalent sound pressure levels. However, they need to be put into the context of the measurement setup, specifically by considering measurement uncertainties. These are partly introduced by the instrumentation, consisting of microphone, sound level meter and calibration equipment [14, 30]. Instrumentation uncertainty for aircraft noise measurements with class 1 measurement equipment was shown to be roughly ±0.5 dB. Other effects, such as local reflections and background noise contamination, can further increase this uncertainty. A detailed study of measurement uncertainties of the NMT network in Zurich and Geneva showed that these additional effects can range from +0.3 dB to +0.9 dB, depending on the location. Together with the location-independent instrumentation uncertainty, the resulting total measurement uncertainty, averaged over all NMTs, is around ±0.9 dB [14, 30].

Based on those uncertainties, we consider mean differences between calculation and measurements of below one decibel as non-significantly different. Mean differences between one and around 2.5 dB can be regarded as good agreement. Differences above 2.5 dB need to be examined closer.

4.2 Full vs. reduced models

Evaluated over all measurements and aircraft types, the simulations reproduced the measurements well. The full models were particularly accurate, with almost all aircraft types matching the measurements with mean differences below one decibel and standard deviations below two decibels (Table 1). It is particularly notable that the approach events with lower noise levels were reproduced very well by the simulation. These events were mostly measured by the additional measurement points A to D in the far range of up to 53 kilometers from touchdown at Zurich airport, where the measured noise levels show an increased variation even for the same aircraft type due to the large influence of configuration changes. The good agreement between simulated and measured levels at those points demonstrates the accurate representation of the full range of aircraft configuration in the full models. All individual full model aircraft types displayed similar performances.

The reduced models achieved similar mean agreement between simulation and measurements as the full models, but with an increase in standard deviation of about 0.7 dB. This increase in uncertainty is partly caused by the models itself: as no FDR data was available for the generation of the reduced models, radar data was used as position information and $N1$ was derived acoustically from the noise measurements [29]. This input data is usually less accurate than FDR data, leading to more inherent uncertainty in the models. During simulation, the lack of FDR data again introduces further uncertainty, since $N1$ has to be approximated using the parameter estimation methodology (see section 2.2). Since the reduced models cannot account for changes in the aircrafts configuration, the simulated noise emissions represent the average configuration settings of the airplane at any given point of the flight. The reduced models are therefore unable to reproduce the differences in noise exposure levels introduced by the real-world configuration variability between individual flights of the same aircraft type. Another factor for the increased uncertainty of the reduced models might be the fact that this group covers a much larger pool of aircraft types operated by different airlines, whereas the full models only represent the comparatively small fleet of Swiss Airlines.

4.2.1 Reduced models in far-range

The influence of the lack of aircraft configuration as input parameters for reduced models could only partially be tested since no measurements in the mid- to far-range, where configuration changes are most prominent, were available. To get an estimate on the increase of uncertainty of the reduced models in the far range, the available measurements of aircraft operated by Swiss Airlines at measurement points A to D were re-evaluated using the reduced version of the full models (*i.e.* the full models without the configuration parameters). This analysis revealed an increase in the standard deviation of roughly 1 dB compared

to the simulation using the full parameter range. Therefore, simulation of approaches in the far-range using reduced models will produce standard deviations that are roughly 1 dB higher than the values listed in Table 2.

Previous analysis on the influence of air absorption under varying weather conditions for far-range propagation let assume that using the approach with a stratified atmosphere described in section 2.1, no significant increase of uncertainty is to be expected as a consequence of the larger propagation distances [31]. As a consequence, the above mentioned increase in uncertainty can be mainly attributed to the lack of aircraft configuration data as input.

4.2.2 Models with poor performance

Most reduced models were able to reproduce the measurements well. There are however three notable exceptions with mean deviations of more than 2.5 dB: The A388_GP7270, the B76X_CF6-80C2 applied to the B762 and the A32X_V2500 applied to the A321. These models need to be investigated further.

The model A388_GP7270 performed poorly upon approach ($\Delta L_{AE,tg}$ = +4.2 ± 3.2 dB). There were no approach measurements available for the Airbus A380 with GP7270 engine for the model generation. Therefore, this model was patched from measurements of the A380 with TRENT9 engine. The validation results suggest that this patch up is not sufficiently accurate.

The model B76X_CF6-80C2 also suffers from the lack of measurements of important routes during the initial measurement campaign, explaining the increased deviations between simulation and measurements seen in Table 2. Furthermore, the validation dataset contained very few measurements of the B762, which further increased the uncertainty of the analyzed level differences.

The B737 family showed good overall results (mean differences < 2.5 dB), but it displays an increase in underestimation of the simulation with increased aircraft size and mass (B737 matches well, B738 was underestimated by up to −1.2 dB, B739 by up to −2.4 dB). While all three types were measured during the initial measurement campaign, the number of measurements per subtype was too small to generate individual emission models. Therefore all measurements were combined to generate a single model for the B737 family. The validation results suggest that the differences in fuselage length and aircraft mass have an unneglectable influence on the noise emission and that one single emission model for an entire aircraft family might therefore not be sufficient.

We suspect the same reason for the poor performance of the model A32X_V2500 when applied to the Airbus A321 at departure ($\Delta L_{AE,tg}$ = −3.2 ± 1.9 dB): the regression dataset of this model mostly consists of measurements of the A319 and A320, leading to an underestimation of noise emissions of the larger and heavier A321.

In contrast to the above types, some models that were derived from measurements of other subtypes within their family worked well. There were no initial measurements available for the Bombardier CRJ7 and CRJX, therefore these types were simulated with the model CRJ9_CF34-8C5 which is entirely based on measurements of the CRJ9. Nevertheless, all three subtypes performed equally well in the validation. The same holds true for the Embraer E195, which was simulated using the E190 emission model and achieved comparable results to the E190 validation.

4.3 Maximum level

The analysis of the maximum levels revealed a a tendency to underestimate the measurements by roughly one decibel. The measured maximum level is highly susceptible to turbulences in the air. Turbulences that occur around the time of shortest source-receiver-distance (direct overflight) can increase the measured maximum level by several decibels, leading to an increase in the averaged maximum level over a large number of measurements. The simulation currently does not take this effect into account, leading to the observed underestimation of the mean $L_{AS,max}$. A distance-dependent correction factor could potentially correct this. However, a corresponding attempt using the original sonAIR source measurements did not yield sufficient correlation. Additional measured level-time histories, together with detailed meteorological data, would be necessary for a final assessment of such a correction factor.

4.4 Sensitivity analysis on input data

The largest influence of changed input data could be identified in the land cover dataset, where the use of coarsely-aggregated data led to a significant overestimation of the simulation. This effect is particularly prominent within settlements, since the coarser dataset does not differentiate between fully reflective areas such as roofs or streets and absorbing surfaces such as parks or gardens.

The vectorized building dataset is exclusively used to calculate shielding effects, making it relevant solely for grazing sound incidence. These situations typically occur

only in the very close vicinity of airports, minimizing the effect on large-scale noise mapping.

The mean differences between the simulations in METEO and BASIC mode were equally insignificant. It has to be noted that the validation explicitly excluded measurements taken during windspeeds of above 5 m/s. Further, the NMT network is set up in a way that there are hardly any measurements of gracing incidences where meteorological effects might play a more prominent role.

4.5 Updated modelling approach

A separation of the calculations by procedure displayed a very good reproduction of approach measurements, while the simulation slightly underestimated the departures. To investigate this underestimation, we further subdivided the departure analysis of the full models by month. This revealed an inter-annual trend with higher underestimation during winter months and better agreement during summer (Figure 5, orange box-whisker-plots).

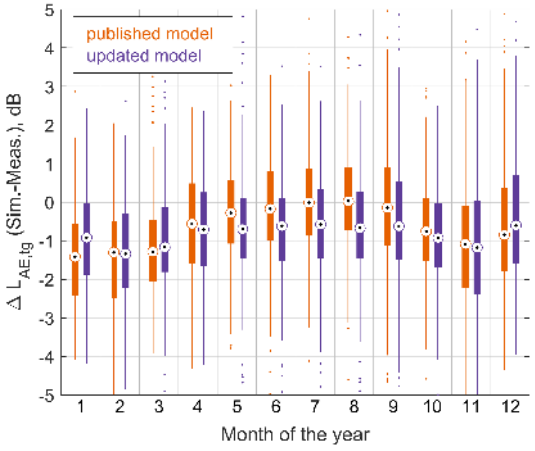

Figure 5: Comparison of inter-annual trends in departure event level differences modelled with published (orange) and updated (purple) full model versions.

This trend correlates with the yearly course of outside air temperatures in Zurich, suggesting that the model does not adequately consider atmospheric conditions during departure. Changes in air temperature and density influence the settings at which the engines are operated as well as the incoming mass flow and jet velocity of the engines, leading to changes in noise emissions. While the parameter $N1$ is able to account for the increase in the engine rotational speed due to higher temperatures and lower air densities, it appears to be insufficient to describe the full extent of influences on noise emissions due to atmospheric changes. Aside from $N1$, the engine noise source term implicitly considers the air temperature with the Mach number Ma, but there is no parameter for the air density in the published modelling approach (Equation 2 in section 2.1). Therefore, a new modelling approach (Equation 12) was developed which extends the engine source term with a variable ρ for the outside air density:

$$\widehat{L}_{0,eng} = L_{e0} + a_{e1} \cdot Ma + b_{e1} \cdot N_1 + b_{e2} \cdot N_1^2 + c_{e1} \cdot \rho \quad (12)$$

The radiation angle terms remain unchanged.

To test this new approach, the full models were recalculated with the extended approach and the validation repeated. The purple box-whisker-plots in Figure 5 show that the new approach somewhat reduced the inter-annual trend in the differences between simulation and measurements. This is partly achieved by reducing the underestimation during the winter months. However, the new approach introduced a new underestimation during summer months. We suspect that this is a consequence of all source measurements for take-off having been carried out during spring and mainly summer months. Therefore the regression dataset does not contain a sufficient range of air densities to adequately predict such a parameter.

Due to the increased underestimation during summer months, the new modelling approach performance is overall slightly poorer than the published approach. The underestimation of the overall $\Delta L_{AE,tg}$ of the engine model is increased by 0.3 dB to -0.8 ± 1.7 dB. An updated release of the published models is therefore not appropriate. However, we expect that models based on measurements covering the full range of air densities (*i.e.* measurements taken over the entire year) would produce better results with the new modelling approach.

5 Conclusion and outlook

The sonAIR aircraft noise simulation model was validated by simulating roughly 20'000 single flights based on real air traffic at Zurich and Geneva airport and comparing the results with the corresponding measurements. The analyzed noise measurements were recorded at 22 locations around the airports, covering a large range of distances between 1.8 and 53 kilometers from the corresponding runways. The validated flights encompass all relevant procedures (departures before and after cutback, approaches with different configurational settings from clean to fully configured, at different flight velocities and altitudes) and all months of the year, therefore representing a large variety of operating

conditions. The analysis over all aircraft types and measurement locations revealed that sonAIR can reproduce the measurements accurately, with mean overall differences for departures as well as approaches of well below ± 1 dB in terms of event levels.

The standard deviation of the simulation depends on the model type: fully parameterized models displayed standard deviations below 2 dB, while the reduced models showed slightly increased uncertainty with standard deviations around 2.5 dB.

The individual full model aircraft types all show similar performances, making them equally applicable for single flight simulations. While most reduced models performed comparably well, there are some that displayed increased uncertainty. Based on the presented validation results, we explicitly discourage the use of three models in their current version for single flight simulations: The B76X_CF6-80C2 for the subtype B762, the A32X_V2500 for the subtype A321 and the A388_GP7270. For all other reduced models, Table 2 should be consulted before using one of them for simulating single flights.

The present analysis revealed that the simulation accuracy strongly depends on the quality and resolution of the used land cover data. We recommend the use of a high-resolution land cover dataset (*e.g.* from official surveying), particularly for noise mapping in densely built-up areas. Other additional input data such as a vectorized building datasets and atmospheric profiles were found to be less critical.

The good performances on single flight simulations suggest that sonAIR is also well suited for calculating entire airport scenarios. To confirm, we are currently carrying out a first test calculation of yearly air traffic at Geneva and Zurich Airport. In addition, a new study at the author's institution is currently repeating the simulation of all flights used in this validation using the simulation models FLULA2 and AEDT. This will allow a direct performance comparison of the different aircraft noise simulation models.

Acknowledgement: The validation of sonAIR was funded by the Federal Office of Civil Aviation (FOCA) and Empa. The authors would also like to thank Swiss International Airlines as well as Zurich and Geneva Airport for their support.

Conflict of Interests: The authors declare no conflict of interest regarding the publication of this paper.

References

[1] ICAO, Recommended Method for Computing Noise Contours Around Airports. Doc 9911, 1st ed. Int Civil Aviat Org (ICAO). Montréal, Canada; 2008.

[2] ECAC. DOC.29: Report on Standard Method of Computing Noise Contours around Civil Airports, Volume 2: Technical Guide, 4th ed., Europ Civil Aviat Conf (ECAC). Neuilly-sur-Seine, France; 2016.

[3] Kontos KB, Janardan BA, Gliebe PR. Improved NASA-ANOPP Noise Prediction Computer Code for Advanced Subsonic Propulsion Systems. Volume 1: ANOPP Evaluation and Fan Noise Model, NASA Lewis Research Center; 1996.

[4] Sanders L, Malbequi P, Legriffon I. Capabilities of IESTA-CARMEN to predict aircraft noise, In: 23rd International Congress on Sound and Vibration (ICSV23). Athens, Greece; 2016.

[5] Van Oosten N. SOPRANO Presentation (PDF). In: SOPRANO Workshop. Madrid, Spain; June 2007.

[6] Bertsch L, Dobrzynski W, Guérin S. Tool Development for Low-Noise Aircraft Design. J Aircr. 2010;47(2):694–9.

[7] Zellmann C, Schäffer B, Wunderli JM, Isermann U, Paschereit CO. Aircraft Noise Emission Model Accounting for Aircraft Flight Parameters. J Aircr. 2017;55(2):682–95.

[8] Zellmann C. Development of an Aircraft Noise Emission Model Accounting for Flight Parameters. PhD thesis. Technische Universität Berlin. Berlin, Germany. 2018.

[9] Wunderli JM, Zellmann C, Köpfli M, Habermacher M, Schwab O, Schlatter F, et al. sonAIR - a GIS-integrated Spectral Aircraft Noise Simulation Tool for Single Flight Prediction and Noise Mapping. Acta Acust United Ac. 2018;104(3):440-451.

[10] Zellmann C, Bertsch L, Schwab O, Wolters F, Delfs J. Aircraft noise assessment of next-generation narrow-body aircraft. In: INTER-NOISE and NOISE-CON Congress and Conference Proc. Madrid, Spain. 2019;259(3):6389–6400.

[11] Rhodes DP, White S, Havelock P. Validating the CAA Aircraft Noise Model with Noise Measurements. Proc Inst Acoust. 2001;23(6):37–44.

[12] Jopson I, Rhodes DP, Havelock P. Aircraft noise model validation - how accurate do we need to be. In: Institute of Acoustics Conference Action on Environmental Noise; 2002:13.

[13] Rhodes DP, Ollerhead JB. Aircraft noise model validation, In: INTER-NOISE and NOISE-CON Congress and Conference Proc. The Hague, The Netherlands. 2001;2:2556-2561.

[14] Thomann G. Mess-und Berechnungsunsicherheit von Fluglärmbelastungen und ihre Konsequenzen. PhD thesis. Eidgenössische Technische Hochschule Zürich. Zurich, Switzerland; 2007 (in German).

[15] Bütikofer R, Thomann G. Validation of FLULA, a time-step model for aircraft noise calculations. In: INTER-NOISE and NOISE-CON Congress and Conference Proc. The Hague, The Netherlands; 2001:927-932.

[16] Bertsch L, Clark IA, Thomas RH, Sanders L, Legriffon I. The Aircraft Noise Simulation Working Group. (ANSWr) – Tool Benchmark and Reference Aircraft Results. In: 25th AIAA/CEAS Aeroacoustics Conference. Delft, Netherlands; 2019. https://doi.org/10.2514/6.2019-2539.

[17] Rizzi S, Legriffon I, Pieren R, Bertsch L. A Comparison of Aircraft Flyover Auralizations by the Aircraft Noise Simulation Working Group. In: AIAA AVIATION 2020 Forum; June 2020.

[18] Jäger D, Zellmann C, Wunderli JM, Simons DG, Snellen M. Validation of the sonAIR Aircraft Noise Simulation Model - a Case Study for Schiphol Airport. In: INTER-NOISE and NOISE-CON Congress and Conference Proc. Chicago, USA. 2018;258(6):1048-1056.

[19] ISO. ISO 9613-1. Acoustics - attenuation of sound during propagation outdoors - Part 1: calculation of the absorption of sound by the atmosphere, International Organization for Standardization. Geneva, Switzerland: ISO; 1993.

[20] Defrance J, Salomons E, Noordhoek I, Heimann D, Plovsing B, Watts G, et al. Outdoor sound propagation reference model developed in the European Harmonoise project. Acta Acust. united Ac., 2007, 93(2), 213-227.

[21] ISO. ISO 9613-2. Acoustics - attenuation of sound during propagation outdoors - Part 2: general method of calculation, International Organization for Standardization. Geneva, Switzerland: ISO; 1996.

[22] Pierce AD. Acoustics. An Introduction to its Physical Principles and Applications. Woodbury, USA: American Institute of Physics; 1991.

[23] Chessell CI. Propagation of noise along a finite impedance boundary. J Acoust Soc Am. 1977;62(4):825–34.

[24] Delany ME, Bazley EN. Acoustical properties of fibrous absorbent materials. Appl Acoust. 1970;3(2):105–16.

[25] Hofmann J., Heutschi K., An engineering model for sound pressure in shadow zones based on numerical simulations, Acta Acust. united Ac., 2005, 91(4), 661–70.

[26] Zellmann C, Jäger D, Schlatter F. Model Adjustment and Validation to Account for the Airflow Deflector Retrofit of the A320 Family, In: 11th European Congress and Exposition on Noise Control Engineering (Euronoise 2018). Crete, Greece. 2018:225–30.

[27] Schwizer P, MacMillan B. New Approaches for the Dynamic Recording of Aircraft Noise as a Basis for Modeling, In: INTER-NOISE and NOISE-CON Congress and Conference Proc. Chicago, USA. 2018;258(6):1576–581.

[28] Schwab O, Zellmann C. Estimation of Flight-Phase-Specific Jet Aircraft Parameters for Noise Simulations. J Aircr. 2020;57(6):1111–20.

[29] Schlüter S, Becker S. Determination of Aircraft Engine Speed Based on Acoustic Measurements, In: INTER-NOISE and NOISE-CON Congress and Conference Proceedings, Hamburg, Germany, 2016, 253(4), 4366-4373.

[30] Bütikofer R, Thomann G. Uncertainty and level adjustments of aircraft noise measurements. In: Proc. of the 2009 International Congress and Exposition on Noise Control Engineering. Ottawa, Canada; 2009.

[31] Zellmann C, Wunderli JM. Influence of the atmospheric stratification on the sound propagation of single flights, In: INTER-NOISE and NOISE-CON Congress and Conference Proc. Melbourne, Australia. 2014;249(4):3770-3779.